

## Optical potential and nuclear deformation for even Nd isotopes from fast neutron scattering

G. Haouat, J. Lachkar, Ch. Lagrange, M. T. McEllistrem,\* Y. Patin, R. E. Shamu,† and J. Sigaud  
*Service de Physique Nucléaire, Centre d'Etudes de Bruyères-le-Châtel, B.P. N° 561, 92542 Montrouge Cedex, France*

(Received 12 February 1979)

Deformation effects in differential cross sections for neutron scattering from  $^{142,144,146,148,150}\text{Nd}$  have been studied at an incident energy of 7 MeV, where measurements and calculations of total cross sections show maximum differences for different deformations. Differential cross sections were obtained for elastic scattering and inelastic scattering to the first  $2^+$  states of the five isotopes. The experimental cross sections are compared to the predictions of surface excitation models using coupled-channels calculations. The parameters of the model are adjusted to fit low energy scattering properties and total cross sections for incident energies from 0.7 to 14 MeV as well as the present data. The large set of data tightly constrains all parameters, including the quadrupole deformation parameters. These are compared to those obtained using other probes of the nuclear surface.

NUCLEAR REACTIONS  $^{142,144,146,148,150}\text{Nd}$  ( $n,n$ ), ( $n,n'$ ),  $E_n=7.0$  MeV measured  $\sigma(E_n, \theta)$ ;  $\theta=20-160^\circ$ ;  $\Delta\theta=5^\circ$ . Enriched targets. Deduced coupled-channels optical potential parameters, quadrupole deformation parameters.

### I. INTRODUCTION

There has recently been much interest in studying the effects of nuclear deformation on neutron scattering. Detailed analyses of measurements of neutron elastic and inelastic scattering from nuclei with  $N=50$  or  $Z=50$  single closed shells<sup>1</sup> from Se isotopes,<sup>2</sup> from nuclei in the rare-earth region,<sup>3,4</sup> and from several actinides<sup>5</sup> have proved that neutrons are powerful probes for investigating nuclear surface properties. These analyses use a nuclear surface deformation formalism for extracting the size of the deformations, and one must make sure that the choice of the optical potential parameters leads to reliable values of the deformation parameters. The basis of the analysis which was developed in a recent study with the  $^{148,150,152,154}\text{Sm}$  isotopes<sup>3</sup> is that an average potential exists which describes neutron scattering for these nuclei at the entrance of the rare-earth region in the absence of deformation effects. Then when these effects are added they can be included through the direct coupling of inelastic scattering channels, the coupling coming through excitation of collective surface vibrations or rotations. A central idea is that the deformation of the nucleus does not alter the scattering potential except as provided by the coupling.<sup>6</sup> In this case the determination of the scattering potential and the deformation parameters, or parameters of the collective excitations, can be separated. The deformation parameters obtained from the analysis are properties of the target nucleus; they do not mask

the changes in the average scattering field. The test of this is the inclusion of both spherical, deformable, and stably deformed nuclei in a common analysis, involving a single complex potential; the only potential changes are those associated with changes of nuclear size and symmetry.<sup>7</sup>

The study reported here is for 7.0 MeV neutron scattering from  $^{142,144,146,148,150}\text{Nd}$ . The advantage of this Nd work is that it includes nuclei which are clearly spherical, including neutron-magic  $^{142}\text{Nd}$ , and  $^{144}\text{Nd}$ . The advantage of the  $^{148-154}\text{Sm}$  study<sup>3</sup> was the inclusion of  $^{152}\text{Sm}$  and  $^{154}\text{Sm}$ , which have several well defined rotational bands at low excitation energies,<sup>8</sup> with  $E2$  transition strengths characteristic of a deformed rotor.<sup>9</sup> But the question of the sphericity of  $^{148}\text{Sm}$  or its susceptibility to deformation was not so clearly answered. The spherical limit may not have been well represented in that study. That  $^{142,144}\text{Nd}$  are spherical is clear from their level spacings at low excitation energies and other information. But that  $^{150}\text{Nd}$  is deformed was not so clear at the beginning of these deformation effect studies. Recent Coulomb excitation studies,<sup>10</sup> however, show a well defined rotational band through at least the  $8^+$  level and transition strengths between levels completely analogous to those in  $^{152}\text{Sm}$ . In fact, the strengths imply average mixing of vibrational bands into the ground state band<sup>10</sup> of the same magnitude as that in  $^{152}\text{Sm}$ .<sup>8</sup> The large range of nuclear structures in these isotopes is evident in Fig. 1, which presents the level scheme of each of them. One sees there the one and two phonon spectra of  $^{146}\text{Nd}$  and

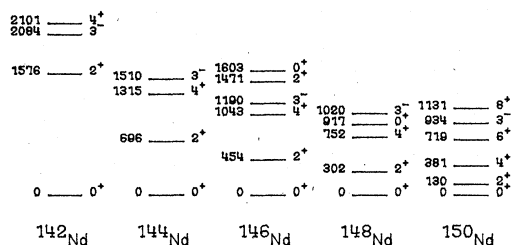


FIG. 1. The low-lying collective states of the even Nd isotopes. Excitation energies are given in keV.

several states of the ground state band of  $^{150}\text{Nd}$ . Five distinct rotational bands are known<sup>9</sup> to exist in  $^{150}\text{Nd}$  within an excitation energy equal to that of the first excited state of semimagic  $^{142}\text{Nd}$ . Thus, evidence from the level schemes and from the  $E2$  transitions correlates to indicate that in these isotopes the full range from spherical to deformed is well represented.

The choice of incident energy 7.0 MeV for the present experiment is in the region in which measurements and calculations<sup>11</sup> show maximum changes in total cross sections ( $\sigma_t$ ) similar to those observed for the Sm isotopes<sup>12</sup> with changes in deformation. It is also an energy high enough so that compound system or statistical model contributions to the excitation of low-lying collective levels are negligible; thus, reaction mechanism ambiguities<sup>13</sup> are avoided. This paper presents an analysis of scattering cross sections similar to that presented<sup>3</sup> for the Sm isotopes, one which couples directly the  $0^+$  and  $2^+$  states through neutron scattering. A preliminary report of the present measurements and a preliminary version of this analysis have already been presented.<sup>14</sup>

## II. EXPERIMENTAL PROCEDURE

The differential cross section measurements were carried out using the four detector neutron time-of-flight facility of the Centre d'Études de Bruyères-le-Châtel. The experimental system used is essentially that described in Ref. 3. Only a brief description of details appropriate to this experiment is presented here. The incident 7.0 MeV neutrons were produced from the  $^2\text{H}(d,n)^3\text{He}$  reaction. The deuteron beam from the tandem accelerator was pulsed and bunched into bursts of 1 ns full width at half maximum (FWHM). The beam entered a 3-cm long deuterium gas target filled at a pressure of 1.3 atm and separated from the evacuated beam extension by a 2.5- $\mu\text{m}$  thick nickel foil. Neutrons were scattered by cylindrical samples located at  $0^\circ$  with respect to the deuteron

beam axis and 13.6 cm from the center of the gas target. The scattered neutrons were detected by an array of four detectors separated from each other by  $20^\circ$ . Each detector consisted of a 12.5-cm diameter, 5-cm thick NE 213 liquid scintillator optically coupled to an XP 1040 photomultiplier tube. The flight path from the sample to each detector was 8.12 m. The total energy spread at the neutron detectors was about 120 keV. This was sufficient to resolve the first excited  $2^+$  state from the ground state easily for  $^{142,144,146,148}\text{Nd}$ . For  $^{150}\text{Nd}$  the 130 keV energy separation of these two states was about the energy resolution; yields for the two scattered neutron groups were separated by line fitting procedures.

The scattering samples consisted of about 40 g of powdered  $\text{Nd}_2\text{O}_3$  and had an isotopic enrichment greater than 94%. The five samples were matched to the same number of molecules (0.112 mole); each of them was contained in a polyethylene container of 2.5 cm diameter and 5.0 cm height. Because the  $\text{Nd}_2\text{O}_3$  powder is quite hygroscopic, it had been carefully dried and then sealed into the polyethylene containers with the powder exposed to air for less than 30 minutes to avoid water contamination. Background time-of-flight runs were made with a water sample and an empty container at each angle in order to subtract oxygen and container peaks from the time-of-flight spectrum.

Yields of scattered neutrons were obtained with eight settings of the four detector array, with seven runs of ~three hours each at each setting. These run durations were sufficient to achieve a precision of better than 3% for elastic scattering at most of the 29 angles between  $20^\circ$  and  $160^\circ$ , with data taken at  $5^\circ$  intervals. The yields from the  $\text{Nd}_2\text{O}_3$ , water, and container were corrected for neutron attenuation, and the corrected background runs were subtracted from the sample runs to provide Nd spectra free of C and O contaminant peaks. The procedure could be tested at back angles, where the C and O peaks were kinematically shifted away from Nd peaks. The subtraction left a clean spectrum, free of statistically significant distortions. Spectra for  $^{148}\text{Nd}$  before and after subtraction of contaminant contributions are shown in Fig. 2 for  $125^\circ$ , at which angle the background was relatively the largest; here the oxygen and  $^{148}\text{Nd}$  differential cross sections are near a local maximum and minimum, respectively. Net yields were obtained by fitting a line to the residual background in the neighborhood of a scattering peak and then adding the yields above the line. Yields were also obtained by fitting standard line shapes to the peaks, to check for consistency of the yield extractions. For  $^{150}\text{Nd}$ , with the ground and first excited states not well resolved, line

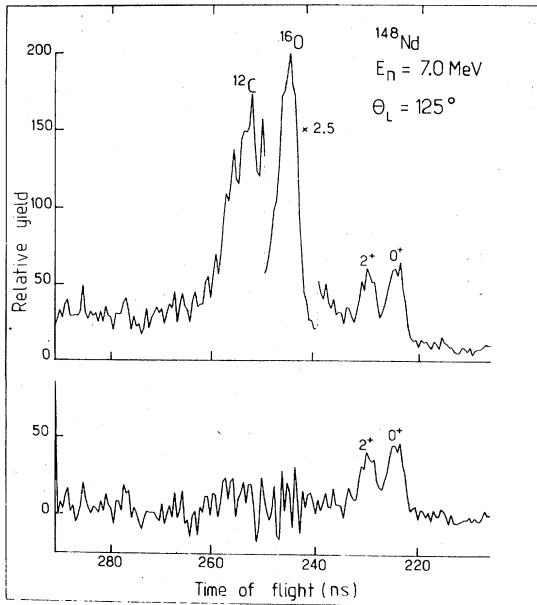


FIG. 2. (a) Time-of-flight spectrum for the  $^{148}\text{Nd}_2\text{O}_3$  sample in a polyethylene container. (b) The same spectrum after subtraction of contaminant contributions.

shapes and the position of the elastic peak were taken from neighboring runs with  $^{146}\text{Nd}$  and  $^{148}\text{Nd}$ . With these constraints, accurate yields for the two  $^{150}\text{Nd}$  groups were easily obtained.

The neutron flux was monitored continuously with a fifth NE213 scintillation detector, also operated in the time-of-flight mode, which viewed the neutron source directly. At regular time intervals the scattering sample was replaced by a calibrated proton recoil counter telescope which subtended the same solid angle at the source as the sample. By comparing the scintillation monitor yield to the flux as determined by the calibrated counter telescope, it was possible to ascertain that the detection efficiency of the time-of-flight monitor had not changed during the course of the rather extended experiment. The energy dependencies of the scintillator detection efficiencies were determined by counting neutrons scattered from hydrogen in a small polyethylene sample and comparing the yields to the well known differential cross sections for  $n$ - $p$  scattering.<sup>15</sup> All scattered yields were corrected for neutron attenuation, multiple scattering, and angular resolution using the analytic method developed by Kinney<sup>16</sup> to approximate the results of Monte Carlo calculations.

Uncertainties of the measurements include those affecting the reproducibility of the measured yields and those associated with normalizing the corrected yields to the known  $n$ - $p$  scattering cross section. The yields have uncertainties associated

with backgrounds, counting statistics, neutron monitor instabilities, and sample positioning. These combine to yield an uncertainty ranging from 2 to 10% for elastic scattering yields. The normalization uncertainty includes contributions from attenuation and multiple scattering corrections and from the energy dependence of the neutron detector efficiency. Altogether they comprise an uncertainty of about 5%.

### III. RESULTS AND ANALYSES

Measured differential scattering cross sections for each of the Nd isotopes studied are presented in Fig. 3 for elastic scattering and in Fig. 4 for inelastic scattering to the first  $2^+$  state; the error bars given include both relative and normalization uncertainties. The curves shown with the data are coupled-channels calculations to be discussed later. Some interesting comparisons can be made directly between these and other measurements. The total cross section differences ( $\Delta\sigma_t$ ) for

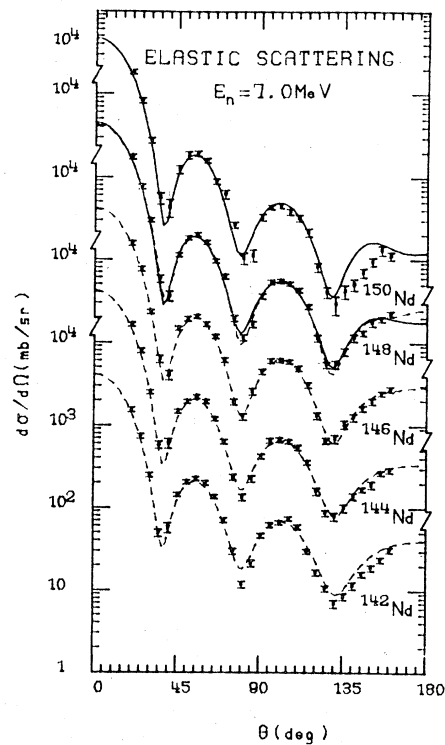


FIG. 3. Differential cross sections for elastic scattering from the even Nd isotopes. The results of coupled-channels calculations are shown as solid lines for the rotational model and as dashed lines for the vibrational model.

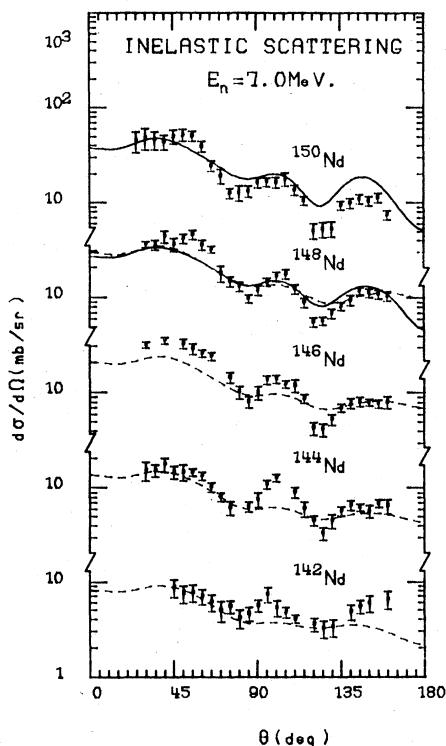


FIG. 4. Inelastic scattering cross sections to the first  $2^+$  level for the Nd isotopes. Solid and dashed lines represent the results of rotational and vibrational coupled-channel calculations, respectively. Note that the calculations have insufficient structure when compared to the data.

$^{142-150}\text{Nd}$  measured by Shamu *et al.*<sup>11</sup> indicate that around 7 MeV the total cross section increases with mass number, or deformation, reaching a difference of 8% between  $^{144}\text{Nd}$  and  $^{150}\text{Nd}$ . Our data show that this increase occurs entirely in the inelastic scattering channels. Only scattering channels are important, since other open channels, such as  $(n, \gamma)$  and  $(n, p)$ , have cross sections too small to contribute significantly. The  $\sigma_t$  and  $\Delta\sigma_t$  are presented in Table I, with  $\Delta\sigma_t \equiv \sigma_t - \sigma_{e1}$  (144),

a difference with respect to the cross section for  $^{144}\text{Nd}$ . Also given in this Table are our angle-integrated cross sections for elastic scattering ( $\sigma_{e1}$ ) and the inelastic scattering to the first  $2^+$  state ( $\sigma_{2+}$ ) of  $^{142-148}\text{Nd}$  and to the first  $2^+$  ( $\sigma_{2+}$ ) and  $4^+$  ( $\sigma_{4+}$ ) states of  $^{150}\text{Nd}$ ; these values are deduced from least-squares fits of Legendre polynomial expansions to the present data. One observes that the values of  $\sigma_{e1}$  are almost the same for the five isotopes, and actually show a slight decrease with increasing mass, of about 1.5 to 2%. Since  $\sigma_{e1}$  is half of  $\sigma_t$ , this affects the total cross section less than 1%. The inelastic scattering cross sections measured ( $\sigma_{in} = \sigma_{2+}$  or  $\sigma_{2+} + \sigma_{4+}$ ), however, show the sharp increase expected with increasing deformation and account for all of the total cross section increase, as is apparent from the comparison of  $\Delta\sigma_t$  with  $\Delta\sigma_{in} \equiv \sigma_{in} - \sigma_{in}^{(144)}$ , a difference with respect to the inelastic cross section for  $^{144}\text{Nd}$ . Implied also in this comparison is the suggestion that the inelastic scattering to all excited levels other than the low-lying collective ones remains almost constant from isotope to isotope.

Another direct comparison which can be made is the one between the cross sections for the three Nd isotopes which are isotones of  $^{148-150}\text{Sm}$ , studied earlier,<sup>3</sup> and the cross sections for those Sm isotopes. For the three isotopes  $^{146,148,150}\text{Nd}$  the average total cross section is  $\sigma_t = 4588$  mb and the average integrated elastic scattering cross section is  $\sigma_{e1} = 2173$  mb. For the isotopes  $^{148,150,152}\text{Sm}$  the corresponding averages are  $\sigma_t = 4565$  mb and  $\sigma_{e1} = 2180$  mb. Isotone pairs have such similar elastic scattering cross sections that the data for both, at 7 MeV incident energy, could be plotted on a single graph, and all of it would seem to belong to a single nucleus.

The elastic scattering changes which are quite striking are those with changing neutron number and for back angle scattering cross sections, whose sharp decrease with increasing deformation was noted in earlier studies.<sup>2-4</sup> This decrease is also shown in Table I for the cross sections integrated over the angular range from  $40^\circ$  to  $160^\circ$

TABLE I. Comparison of neutron total, elastic and inelastic scattering cross sections at 7.0 MeV for the Nd isotopes.

Isotope	$\sigma_t^a$ (mb)	$\sigma_{e1}$ (mb)	$\sigma_{e1}$ (40-160) (mb)	$\sigma_{2+}$ (mb)	$\sigma_{4+}$ (mb)	$\Delta\sigma_{in}$ (mb)	$\Delta\sigma_t^a$ (mb)
$^{142}\text{Nd}$	$4362 \pm 62$	$2200 \pm 114$	$720 \pm 50$	$68 \pm 8$	$\approx 0$	$-42 \pm 11$	$-49 \pm 33$
$^{144}\text{Nd}$	$4411 \pm 52$	$2252 \pm 90$	$693 \pm 48$	$110 \pm 8$	$\approx 0$	0	0
$^{146}\text{Nd}$	$4509 \pm 63$	$2146 \pm 128$	$643 \pm 50$	$201 \pm 9$	$\approx 0$	$91 \pm 12$	$98 \pm 34$
$^{148}\text{Nd}$	$4545 \pm 63$	$2206 \pm 125$	$578 \pm 46$	$237 \pm 17$	$\approx 0$	$127 \pm 19$	$134 \pm 34$
$^{150}\text{Nd}$	$4711 \pm 63$	$2167 \pm 169$	$529 \pm 60$	$265 \pm 18$	$168 \pm 28$	$323 \pm 46$	$300 \pm 34$

<sup>a</sup>Reference 11.

$[\sigma_{01}(40-160)]$ , beyond the forward peak. Thus, to keep the whole angle-integrated cross section approximately constant, the forward angle cross sections must increase markedly with deformation, and they do, approximately as the square of the increasing total cross section. In fact, the extrapolated zero degree cross sections are consistent with Wick's limit,<sup>17</sup> which is proportional to  $\sigma_t^2$ . All of these changes and the large inelastic scattering cross sections were well represented in a coupled-channels analysis for the Sm isotopes.<sup>3</sup> Theoretical calculations to fit the present results were in the same model, with the Nd isotopes treated as nuclei very similar to each other except for changes in deformation in going from <sup>142</sup>Nd to <sup>150</sup>Nd. The analysis was again carried out using the coupled-channels nonspherical potential formalism of Tamura.<sup>18</sup> The real and imaginary parts of the potential included the usual energy and isospin dependencies,<sup>7</sup> but other than that they were the same for all isotopes.

The actual potential parameters used in this analysis were obtained by means of the method described in Ref. 19, which avoids parameter ambiguities often encountered in scattering analyses. It requires a consistent representation of scattering properties over the whole energy range from 10 keV to 14 MeV. The data set which was used included these 7.0 MeV scattering data, cross sections for the same nuclei measured in this laboratory for 4.08 MeV neutrons incident,<sup>20</sup> total cross sections and total cross section differences,<sup>11</sup> and the very low energy scattering properties. These last properties include the *s*- (Ref. 21) and *p*-wave<sup>22,23</sup> strength functions and the scattering length.<sup>24</sup> This analysis, based as it is on so many scattering properties in addition to the present data, gives us confidence that the scattering potential parameters and the deformation parameters are well determined. Values of the potential parameters thus deduced are

$$\left. \begin{aligned} V &= 50.17 - 18.00(N-Z)/A - 0.22 E_n, \\ W_D &= 4.66 - 9.00(N-Z)/A + 1.10\sqrt{E_n} \\ W &= 0 \end{aligned} \right\} \text{for } E_n \leq 8 \text{ MeV,}$$

$$\left. \begin{aligned} W_D &= 7.77 - 9.00(N-Z)/A - 0.05 E_n \\ W &= -1.28 + 0.16 E_n \end{aligned} \right\} \text{for } E_n > 8 \text{ MeV,}$$

and  $V_{s_0} = 8.50$ ,

where all potential strengths and neutron energies are in MeV and

$$a = 0.65, \quad \bar{a} = 0.58, \quad \text{and } R_0 = \bar{R}_0 = 1.25 A^{1/3},$$

with all geometric parameters in fm (see Ref. 18 for the notation).

A modified version<sup>25</sup> of Tamura's code<sup>26</sup> JUPITOR 1 was used for the calculations. Only quadrupole deformations for the nuclear potential were considered here. The calculations were performed with the coupling basis  $(0^+, 2^+)$ , assuming complex form factors; the spin-orbit potential was not deformed and did not contribute to the coupling. The quadrupole deformation parameter  $\beta_2$  was the only variable from isotope to isotope. The nucleus <sup>150</sup>Nd was treated as a rigid rotor, whereas the nuclei <sup>142,144,146</sup>Nd were considered as spherical vibrators. For <sup>148</sup>Nd no clear indication of its structural character or shape is available<sup>27,28</sup>; therefore, both vibrational and rotational calculations were performed.

The energy dependencies of the real and imaginary parts of the potential given above are slightly different from those used earlier,<sup>3</sup> in order to accommodate the new data set at 4.08 MeV incident energy,<sup>20</sup> and also provide a good representation for the 7.0 MeV data. Nonetheless, the real potential strengths are almost the same for Nd and Sm. But the imaginary potential depth for Nd is slightly stronger than for Sm, if indeed this difference is significant at all. The very low energy scattering properties found for the Nd isotopes are compared to measurements in Table II, and the agreement shown there is rather satisfactory. The deformation parameters are tightly constrained to the values given in Table III, and compared there to the values found earlier<sup>3</sup> for the Sm isotopes. One sees almost the same values for Nd and Sm isotones, as one might have expected on the basis of the very similar elastic scattering and total cross sections demonstrated above.

Our work on the Nd isotopes at 4.08 MeV has indicated that, at that energy, compound nucleus (CN) contributions can be substantial.<sup>20</sup> The Wolfenstein-Hauser-Feshbach formalism was employed to calculate CN contributions to elastic and inelastic scattering for <sup>142,144,146,148,150</sup>Nd. Allowances were made for resonance width fluctuations.<sup>29</sup> As one would expect, CN effects were largest for neutron-magic <sup>142</sup>Nd.<sup>20</sup> In the present work, CN calculations similar to those described above were performed at 7 MeV. The CN contribution to the scattering was found to be negligible for both the elastic scattering and the inelastic scattering to the first  $2^+$  state in all nuclei. The maximum effect was 1% for the  $2^+$  state cross section of the neutron closed-shell <sup>142</sup>Nd. Since, to first order,<sup>18</sup>  $\beta_2 \propto (\sigma_{2+})^{1/2}$ , this means that the error in our  $\beta_2$  for <sup>142</sup>Nd, the worst case, would be about 0.5%. The details for our CN calculations

TABLE II. Comparison of experimental values of low-energy neutron scattering parameters with calculated values at 10 keV for Nd.

Parameter	<sup>142</sup> Nd		<sup>144</sup> Nd		<sup>146</sup> Nd		<sup>148</sup> Nd		<sup>150</sup> Nd	
	Exp.	Calc.	Exp.	Calc.	Exp.	Calc.	Exp.	Calc.	Exp.	Calc.
$S_0(\times 10^4)$	$1.4 \pm 0.4^a$	2.25	$3.9 \pm 1.0^a$	2.85	$2.3 \pm 0.6^a$	3.77	$3.0 \pm 0.6^a$	5.16(rot.) 5.04(vib.)	$3.2 \pm 0.6^a$	2.77
$S_1(\times 10^4)^b$	$1.0 \pm 0.4^c$	1.73	$0.8 \pm 0.8^d$	1.73	$0.8 \pm 0.8^d$	1.98	$0.8 \pm 0.8^d$	1.80(rot.) 2.32(vib.)	$0.8^d$	1.67
$R'$ (fm)		4.33	$7.6 \pm 3.0^e$	4.42	$8.7 \pm 3.4^e$	4.75	$8.2 \pm 3.1^e$	8.12(rot.) 5.71(vib.)		8.15

<sup>a</sup>Reference 21.<sup>b</sup>We assumed  $a_c = 1.25 A^{1/3}$  for the channel radius.<sup>c</sup>Reference 22.<sup>d</sup>Reference 23.<sup>e</sup>Reference 24.

will be presented elsewhere.<sup>20</sup>

The calculated differential scattering cross sections are displayed in Figs. 3 and 4 as dashed and full curves for the vibrational and rotational types of collective coupling, respectively. The agreement shown in Fig. 3 between calculations and measurements for elastic scattering is excellent; there are slight discrepancies beyond 130° only for <sup>142</sup>Nd and <sup>150</sup>Nd. For <sup>150</sup>Nd these discrepancies cannot be ascribed to an unreliable separation of the elastic and inelastic (2<sup>+</sup>) neutron groups since the measured composite cross sections, presented in Fig. 5, are still smaller than the corresponding calculated values at backward angles. The fits to the inelastic scattering to the first 2<sup>+</sup> level shown in Fig. 4 are not as uniformly excellent as for the elastic scattering, but still give a quite good representation of the measurements. The general shape of the angular distribution is reproduced, and the average cross section, which depends sensitively on the magnitude of the deformation parameter  $\beta_2$ , is also well fitted for each nuclide. The calculated curve for <sup>148</sup>Nd with the rigid rotor model has more structure, and thus better represents the data, than that for the vibrational model. The elastic scattering calcula-

tions for <sup>148</sup>Nd with the two models are almost identical. The general failure of these models in reproducing such details as the amount of structure in the inelastic scattering angular distributions has been pointed out before,<sup>3</sup> and is a point strongly confirmed in this experiment, as is evident in Fig. 4. However, Brieva and Georgiev<sup>30</sup> have recently shown that by using a realistic scattering potential they could obtain more structure in the cross sections for inelastic scattering to the first 2<sup>+</sup> state of <sup>152</sup>Sm at 7 MeV. They used in their coupled-channels calculations a nucleon-nucleus optical potential which was essentially obtained by folding an effective nucleon-nucleon interaction with the density distribution describing the deformed target nucleus; they included exchange effects.

Although the  $\Delta\sigma_t$  studies<sup>11,12</sup> indicated strong deformation effects as low as 2.5 MeV incident energy and neutron scattering from Sm isotopes,<sup>13</sup> also at 2.5 MeV were shown to be quite susceptible to nuclear deformation, the sensitivity with which the coupling parameter  $\beta_2$  can be fixed is probably best near 7 MeV. At low energies the analysis is complicated by the fact that both direct interaction (DI) and compound nucleus contributions are im-

TABLE III. Deformation parameters  $\beta_2$  derived in this experiment for the Nd isotopes. Also given for comparison are the  $\beta_2$  values for the Sm isotopes (Refs. 3, 12, and 20). The associated uncertainties are believed to be  $\pm 5\%$ .

Z \ N	N					
	82	84	86	88	90	92
60 Nd	142	144	146	148	150	
$\beta_2$	0.10	0.12	0.15	0.18	0.21	
62 Sm			148	150	152	154
$\beta_2$			0.13	0.17	0.22	0.24

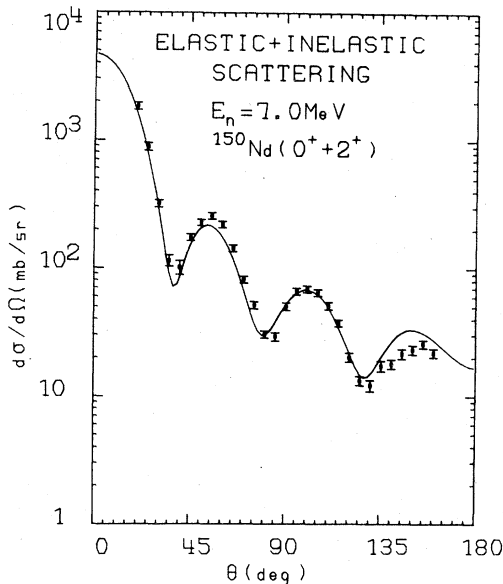


FIG. 5. Measurements and calculations of the composite cross sections for both the ground state ( $0^+$ ) and the first excited  $2^+$  state of  $^{150}\text{Nd}$ .

portant. Moreover, the CN cross sections, which are nearly nuclear dynamics independent, are difficult to determine since they depend on the distributions and correlations of the level partial widths.<sup>29</sup> On the other hand, at 7 MeV the CN and DI excitations are completely separated in the excitation spectrum of the target.

The present work together with the earlier Sm study<sup>3</sup> demonstrate that deformation effects are quite strong in elastic and inelastic scattering, and that a coupled-channels analysis provides a good, neutron energy independent parametrization of all scattering properties. The comparison of the currently determined  $\beta_2$  values with those from the Sm study in Table III shows that in this mass region of transition from spherical to deformed shapes the quadrupole deformation parameter is very similar for isotones; hence  $\beta_2$  seems to depend most on neutron number.

Since the nuclear shape parameters are well fixed by fitting the present data as well as other scattering data<sup>20</sup> and total cross sections over an extended range of neutron energy,<sup>11</sup> we can compare them to determinations from Coulomb excitation and other nuclear excitation experiments. But the charge deformation parameters and the nuclear deformation parameters may not be really equivalent.<sup>31,32</sup> Moreover, the nuclear deformation parameters cannot be directly compared among themselves because of the different sizes

of the bombarding projectiles. However, as has been pointed out, the deformation lengths from different excitation methods should be comparable. It is actually this quantity which determines the strength of coupling between the  $0^+$  and  $2^+$  levels. Values of the quadrupole deformation length  $\beta_2 R_0$  obtained in the present study are given in Table IV along with other deformation lengths deduced from Coulomb excitation,<sup>33-36</sup> inelastic electron scattering,<sup>37</sup> and inelastic scattering of heavy ions in the energy region of interference between Coulomb and nuclear excitation.<sup>38,39</sup>

Recently, a careful determination of Coulomb and nuclear excitation parameters was completed for  $^{142}\text{Nd}$  by Thornton *et al.*<sup>38</sup> using  $^{13}\text{C}$  ions. They found that distorted-wave Born-approximation (DWBA) calculations gave almost equal values of the Coulomb and nuclear deformation lengths for the first  $2^+$  level. This equality is confirmed by the good agreement, observed in Table IV, between these values, the Coulomb excitation data, and the nuclear deformation length obtained in the present analysis. On the other hand Hillis *et al.*,<sup>39</sup> in a study of scattering of  $^{12}\text{C}$  ions from the five even Nd isotopes, found that a single-step DWBA analysis failed to fit their data. Their data were then successfully described when they performed coupled-channels calculations which included strong two-step processes such as quadrupole reorientation in the case of the first  $2^+$  state excitation. For these latter calculations they assumed equal deformation lengths for Coulomb and nuclear excitation. Thus there seems to be some ambiguity in the results from heavy ion experiments, with rather strong dependence<sup>39</sup> on poorly known matrix elements.

Nuclear charge deformation lengths were also deduced from reduced transition probabilities  $B(E2, 0^+ \rightarrow 2^+)$  measured in Coulomb excitation experiments. Deformation lengths were computed assuming homogeneous charge distributions. For the isotopes  $^{142,144,146,148}\text{Nd}$  (Table IV, columns 5 to 8), we used the relationship

$$\beta_2 R_0 = \frac{4\pi}{3ZR_0} [B(E2)]^{1/2}, \quad (1)$$

where  $Z$  is the atomic number and  $R_0 = 1.2A^{1/3}$  fm is the nuclear charge radius. For large values of  $\beta_2$ , Eq. (1) is not strictly correct since higher order terms in  $\beta_2$  must be included in the left-hand side of the equation.<sup>40</sup> In addition, an hexadecapole deformation ( $\beta_4$ ) should be taken into account. Performing a calculation including both  $E2$  and  $E4$  transitions for  $^{150}\text{Nd}$ , Wollersheim and Elze<sup>33</sup> have derived the deformation parameters  $\beta_2$  and  $\beta_4$  from

TABLE IV. Quadrupole deformation length  $\beta_2 R_0$  deduced from the present analysis in comparison with data obtained from previous electromagnetic excitation and Coulomb-nuclear interference experiments.

Isotope	Nuclear excitation ( $n, \pi'$ )	Coulomb-nuclear interference		Electromagnetic excitation				
		Thornton <i>et al.</i> (Ref. 38) ( $^{13}\text{C}, ^{13}\text{C}'$ )	Hillis <i>et al.</i> (Ref. 39) ( $^{12}\text{C}, ^{12}\text{C}'$ )	Eccleshall <i>et al.</i> (Ref. 34) ( $^{16}\text{O}, ^{16}\text{O}'$ )	Crowley <i>et al.</i> (Ref. 35) ( $^{16}\text{O}, ^{16}\text{O}'$ )	Nathan and Popov (Ref. 36) ( $\alpha, \alpha'$ )	Madsen <i>et al.</i> (Ref. 37) ( $e, e'$ )	Wollersheim and Elze (Ref. 33) ( $\alpha, \alpha'$ )
$^{142}\text{Nd}$	$0.65 \pm 0.03$	$0.56^a$ $0.59^b$	$0.63^c$	$0.72^d$	$0.65^d$	$0.60^d$		
$^{144}\text{Nd}$	$0.79 \pm 0.04$		$0.67^c$	$0.74^d$	$0.79^d$			
$^{146}\text{Nd}$	$0.99 \pm 0.05$		$0.99^c$	$0.89^d$	$0.96^d$	$0.93^d$		
$^{148}\text{Nd}$	$1.19 \pm 0.06$		$1.23^c$	$1.07^d$	$1.28^d$			
$^{150}\text{Nd}$	$1.40 \pm 0.07$		$1.71^c$					$1.57^e$

<sup>a</sup>Nuclear deformation length.

<sup>b</sup>Charge deformation length.

<sup>c</sup>Results of coupled-channels calculations for which the deformation length has been taken equal for both Coulomb and nuclear excitations.

<sup>d</sup>Values deduced from the reduced transitions probabilities  $B(E2)$  by using Eq. 2 in the text.

<sup>e</sup>Value deduced from the analysis of Ref. 33.

their measurements of the reduced transition matrix elements

$$M_{02} \equiv \langle 2^+ \| M(E2) \| 0^+ \rangle$$

and

$$M_{04} \equiv \langle 4^+ \| M(E4) \| 0^+ \rangle.$$

The deformation length obtained in their study is given in Table IV. The  $M_{02}$  value found by these authors<sup>33</sup> is in excellent agreement with those deduced from various other works.<sup>10,41</sup>

### CONCLUSIONS

This study of neutron scattering in five Nd isotopes confirms and extends observation of the marked effects of deformation-induced coupling between neutron scattering channels. Strong effects of deformation on neutron elastic scattering angular distributions, reported earlier for a few Sm isotopes, are now extended to these Nd isotopes. Perhaps most remarkable is the range of applicability of coupled-channels analyses using simple collective excitation models of the coupling, which appear to apply to nuclei ranging from neutron-magic  $^{142}\text{Nd}$  to the rigid rotor  $^{154}\text{Sm}$ . When the different nuclear structure properties of these very different nuclei are accommodated in the coupled-channels model, a single scattering potential describes the scattering from all of them.

One defect of these surface excitation coupled-channels models had been noted for inelastic scattering to the first  $2^+$  level of  $^{152}\text{Sm}$ . The measured angular distribution for inelastic scattering showed more structure than did the calculation. We see that same detailed deficiency recur for scattering in these isotopes, suggesting a minor unresolved problem in the detailed character of these coupled-channels analyses which could be overcome by using a more realistic optical potential than a deformed Saxon-Woods parametrization.

Nevertheless, the sensitivity of the scattering to deformations and the values of deformation lengths extracted suggest that neutron scattering is a sensitive and reliable method of measuring the susceptibility of the nuclei to  $E2$  excitation, provided that the analysis includes low energy scattering properties as well as the total cross sections and differential cross sections for elastic and inelastic scattering.

We wish to thank Dr. A. Michaudon for his continued support and encouragement in these rare-earth studies. It is a pleasure to acknowledge



many informative discussions with D. Gogny and M. Girod about the structures of the Nd isotopes. We thank J. P. Delaroche for his assistance with some details of the analysis. Finally, we thank

the USERDA for the loan of the Nd<sub>2</sub>O<sub>3</sub> separated isotope samples and the Western Michigan University Faculty Research Fund for financial assistance with the loan.

- \*On leave from the University of Kentucky. Present address: University of Kentucky, Lexington, Kentucky, 40506.
- †On leave from Western Michigan University. Present address: Western Michigan University, Kalamazoo, Michigan, 49001.
- <sup>1</sup>D. E. Bainum, R. W. Finlay, J. Rapaport, J. D. Carlson, and J. R. Comfort, *Phys. Rev. Lett.* **39**, 443 (1977).
- <sup>2</sup>J. Lachkar, M. T. McEllistrem, G. Haouat, Y. Patin, J. Sigaud, and F. Coğu, *Phys. Rev. C* **14**, 933 (1976).
- <sup>3</sup>M. T. McEllistrem, R. E. Shamu, J. Lachkar, G. Haouat, Ch. Lagrange, Y. Patin, J. Sigaud, and F. Coğu, *Phys. Rev. C* **15**, 927 (1977).
- <sup>4</sup>Ch. Lagrange, R. E. Shamu, T. Burrows, G. P. Glasgow, G. Hardie, and F. D. McDaniels, *Phys. Lett.* **58B**, 293 (1975).
- <sup>5</sup>A. T. G. Ferguson, I. J. Van Heerden, P. Moldauer, and A. B. Smith, in *Proceedings of the International Conference on the Interactions of Neutrons with Nuclei*, University of Lowell, Lowell, Massachusetts, 1976, edited by Eric Sheldon (ERDA, Oak Ridge, 1976), p. 204; G. Haouat, J. Sigaud, J. Lachkar, Ch. Lagrange, B. Duchemin, and Y. Patin, Report No. INDF(FR) 13/L, 1977 (unpublished); G. Haouat, J. Lachkar, Ch. Lagrange, Y. Patin, J. Sigaud, and R. E. Shamu, Report No. INDF(FR) 29/L, 1978 (unpublished).
- <sup>6</sup>N. K. Glendenning, D. L. Hendrie, and O. N. Jarvis, *Phys. Lett.* **26B**, 131 (1968).
- <sup>7</sup>C. M. Perey and F. G. Perey, *At. Data Nucl. Data Tables* **17**, 2 (1976); M. T. McEllistrem, in *Proceedings of the International Conference on the Interactions of Neutrons with Nuclei*, University of Lowell, Lowell, Massachusetts, 1976, edited by Eric Sheldon (ERDA, Oak Ridge, 1976), Vol. 1, p. 171.
- <sup>8</sup>L. L. Riedinger, Noah R. Johnson, and J. H. Hamilton, *Phys. Rev.* **179**, 1214 (1969); L. Varnell, J. D. Bowman, and J. Trischuk, *Nucl. Phys.* **A127**, 270 (1969); J. H. Hamilton, F. E. Coffman, A. V. Ramaya, and K. Baker, *Phys. Rev. C* **3**, 960 (1971).
- <sup>9</sup>R. O. Sayer, P. H. Stelson, F. K. McGowan, W. T. Milner, and R. L. Robinson, *Phys. Rev. C* **1**, 1525 (1970); R. M. Diamond, F. S. Stephens, K. Nakai, and R. Nordhagen, *ibid.* **3**, 344 (1971); A. H. Shaw, and J. S. Greenberg, *ibid.* **10**, 263 (1974); J. M. Domingos, G. D. Symons, and A. C. Douglas, *ibid.* **10**, 250 (1974); F. Fischer, D. Kamke, H. J. Kittling, E. Kuhlmann, H. Plicht, and R. Shormann, *ibid.* **15**, 921 (1977).
- <sup>10</sup>S. W. Yates, Noah R. Johnson, L. L. Riedinger, and A. C. Kahler, *Phys. Rev. C* **17**, 634 (1978), and references cited therein.
- <sup>11</sup>R. E. Shamu, E. M. Bernstein, and Ch. Lagrange, *Bull. Am. Phys. Soc.* **20**, 1196 (1975).
- <sup>12</sup>R. E. Shamu, Ch. Lagrange, E. M. Bernstein, J. J. Ramirez, T. Tamura, and C. Y. Wong, *Phys. Lett.* **61B**, 29 (1976).
- <sup>13</sup>D. F. Coope, M. C. Schell, S. N. Tripathi, and M. T. McEllistrem, *Phys. Rev. Lett.* **37**, 1126 (1976); D. F. Coope, S. N. Tripathi, M. C. Schell, J. L. Weil, and M. T. McEllistrem, *Phys. Rev. C* **16**, 2223 (1977).
- <sup>14</sup>G. Haouat, J. Lachkar, Ch. Lagrange, M. T. McEllistrem, Y. Patin, R. E. Shamu, and J. Sigaud, *Bull. Am. Phys. Soc.* **20**, 1196 (1975).
- <sup>15</sup>J. C. Hopkins and G. Breit, *Nucl. Data* **A9**, 137 (1971).
- <sup>16</sup>W. E. Kinney, *Nucl. Instrum. Methods* **83**, 15 (1970).
- <sup>17</sup>G. C. Wick, *Phys. Rev.* **75**, 1459 (1949).
- <sup>18</sup>T. Tamura, *Rev. Mod. Phys.* **37**, 679 (1965).
- <sup>19</sup>J. P. Delaroche, Ch. Lagrange and J. Salvy, Meeting on the use of Nuclear Theory in neutron nuclear data evaluation, Report No. IAEA-190, 1976 (unpublished), p. 251.
- <sup>20</sup>R. E. Shamu, G. Haouat, J. Lachkar, M. T. McEllistrem, Ch. Lagrange, J. Sigaud, J. P. Delaroche, Y. Patin, and F. Coğu, in *Proceedings of the International Conference on the Interactions of Neutrons with Nuclei*, Lowell, Mass., 1976, edited by E. Sheldon (ERDA, Oak Ridge, 1976), p. 1327.
- <sup>21</sup>*Resonance Parameters*, compiled by S. F. Mughabghab and D. I. Garber, BNL, Report No. BNL-325 (National Technical Information Service, Springfield, Virginia, 1973), 3rd ed., Vol. 1.
- <sup>22</sup>J. Boldeman, private communication.
- <sup>23</sup>W. Pineo, Ph.D. dissertation, Duke University, 1970 (unpublished).
- <sup>24</sup>W. Pineo, H. Divadeenam, E. G. Bilpuch, K. Seth, and H. W. Newson, *Ann. Phys. (N.Y.)* **84**, 165 (1974).
- <sup>25</sup>Ch. Lagrange and N. Mondon, *Internal Report*, Centre d'Etudes de Limeil, France, 1973 (unpublished).
- <sup>26</sup>T. Tamura, ORNL Report No. ORNL 4152, 1967 (unpublished).
- <sup>27</sup>P. Carlos, H. Beil, R. Bergère, A. Lepretre, and A. Veysière, *Nucl. Phys.* **A172**, 437 (1971).
- <sup>28</sup>O. V. Vasilijev, G. N. Zalesny, S. F. Semenko, and V. A. Semenov, *Phys. Lett.* **30B**, 97 (1969).
- <sup>29</sup>P. A. Moldauer, *Phys. Rev. C* **11**, 426 (1975); Argonne National Laboratory Report No. ANL/NDM-40, 1978 (unpublished).
- <sup>30</sup>F. A. Brieva and B. Z. Georgiev, *Nucl. Phys.* **A308**, 27 (1978).
- <sup>31</sup>D. L. Hendrie, N. K. Glendenning, B. G. Harvey, O. N. Jarvis, H. H. Duhm, J. Saudinos, and J. Mahoney, *Phys. Lett.* **26B**, 127 (1968).
- <sup>32</sup>D. L. Hendrie, *Phys. Rev. Lett.* **31**, 478 (1973).
- <sup>33</sup>H. J. Wollersheim and Th. W. Elze, *Nucl. Phys.* **A278**, 87 (1977).
- <sup>34</sup>D. Eccleshall, M. J. L. Yates, and J. J. Simpson, *Nucl. Phys.* **78**, 481 (1966).
- <sup>35</sup>P. A. Crowley, J. R. Kerns, and J. X. Saladin, *Phys. Rev. C* **3**, 2049 (1971).
- <sup>36</sup>O. Nathan and V. I. Popov, *Nucl. Phys.* **21**, 631 (1960).

- <sup>37</sup>D. W. Madsen, L. S. Cardman, J. R. Legg, and C. K. Bockelman, Nucl. Phys. A168, 97 (1971).
- <sup>38</sup>S. T. Thornton, T. C. Schweizer, and D. E. Gustafson, Nucl. Phys. A270, 428 (1976).
- <sup>39</sup>D. L. Hillis, E. E. Gross, D. C. Hensley, C. R. Bingham, F. T. Baker, and A. Scott, Phys. Rev. C 16, 1467 (1977).
- <sup>40</sup>P. H. Stelson and L. Grodzins, Nucl. Data A1, 21 (1965).
- <sup>41</sup>J. Bjerregard, B. Elbek, O. Hansen, and P. Salling, Nucl. Phys. 44, 280 (1963); J. D. Kurfess and R. P. Scharenberg, Phys. Rev. 161, 1185 (1967); F. W. Richter, J. Schütt, and D. Wiegandt, Z. Phys. 213, 202 (1968); M. Birk, G. Goldring, and Y. Wolfson, Phys. Rev. 116, 730 (1959); H. S. Gertzman, D. Cline, H. E. Gove, and P. H. S. Lesser, Nucl. Phys. A151, 282 (1970).